Neurobiology of Disease 125 (2019) 77–91

Contents lists available at ScienceDirect

Neurobiology of Disease

journal homepage: www.elsevier.com/locate/ynbdi

N-Palmitoylethanolamine-oxazoline (PEA-OXA): A new therapeutic strategy to reduce neuroinflammation, oxidative stress associated to vascular dementia in an experimental model of repeated bilateral common carotid arteries occlusion

Daniela Impellizzeri[a], Rosalba Siracusa[a], Marika Cordaro[a], Rosalia Crupi[a], Alessio Filippo Peritore[a], Enrico Gugliandolo[a], Ramona D'Amico[a], Stefania Petrosino[b,c], Maurizio Evangelista[d], Rosanna Di Paola[a], Salvatore Cuzzocrea[a,e,*]

[a] Department of Chemical, Biological, Pharmaceutical and Environmental Science, University of Messina, Messina, Italy
[b] Endocannabinoid Research Group, Istituto di Chimica Biomolecolare, Consiglio Nazionale delle Ricerche, Via Campi Flegrei 34, 80078, Pozzuoli, Napoli, Italy
[c] Epitech Group SpA, Via Einaudi 13, 35030, Saccolongo, Padova, Italy
[d] Institute of Anaesthesiology and Reanimation, Catholic University of the Sacred Heart, Rome, Italy
[e] Department of Pharmacological and Physiological Science, Saint Louis University School of Medicine,Saint Louis, USA

ARTICLE INFO

Keywords:
Neuroprotection
Palmitoylethanolamide
Oxazoline
Oxidative stress
Inflammation

ABSTRACT

Aim: Recent studies revealed that pharmacological modulation of NAE-hydrolyzing acid amidase (NAAA) can be achieved with PEA oxazoline (PEA-OXA). Hence, the aim of the present work was to thoroughly evaluate the anti-inflammatory and neuroprotective effects of PEA-OXA in an experimental model of vascular dementia (VaD) induced by bilateral carotid arteries occlusion. At 24 h after VaD induction, animals were orally administered with 10 mg/kg of PEA-OXA daily for 15 days.

Results: Brain tissues were handled for histological, immunohistochemical, western blot, and immunofluorescence analysis. PEA-OXA treatment evidently reduced the histological alterations and neuronal death induced by VaD and additionally improved behavioral deficits. Further, PEA-OXA decreased GFAP and Iba-1, markers of astrocytes, and microglia activation, as well as increased MAP-2, a marker of neuron development. Moreover, PEA-OXA reduced oxidative stress, modulated Nrf2-mediated antioxidant response, and inhibited the apoptotic process.

Innovation: Some drugs may demonstrate their healing potential by regulating neuroinflammation, rather than by their habitually attributed actions only. Palmitoylethanolamide (PEA) is a prototype ALIAmide, well-known for its analgesic, anti-inflammatory, and neuroprotective properties. The inhibition of PEA degradation by targeting NAAA, its catabolic enzyme, is a different approach for treating neuroinflammation. This research offers new insight into the mechanism of PEA-OXA-induced neuroprotection.

Conclusion: Thus, the modulation of intracellular NAAA by PEA-OXA could offer a novel means of controlling neuroinflammatory conditions associated with VaD.

1. Introduction

Vascular dementia (VaD) is the second cause of dementia, after Alzheimer's disease (AD) (Choi et al., 2011). It can be aggravated by a multiplicity of causes, including cerebrovascular dysfunction. The principal risk factors of VaD are obesity, insulin resistance, diabetes,

Abbreviations: AD, Alzheimer's disease; ALIA, Autacoid local inflammation antagonism; CAR, Carrageenan; CNS, Central nervous system; Keap1, Kelch-like ECH associating protein 1; MC, Mast-cell; MWM, Morris water maze; NAEs, N-acylethanolamines; PEA-OXA, N-Palmitoylethanolamine-oxazoline; NAAA, NAE-hydrolyzing acid amidase; NOR, Novel object recognition test; (NF)-κB, Nuclear factor; Nrf2, Nuclear factor erythroid 2 related factor 2; PEA, Palmitoylethanolamide; ROS, Reactive oxygen species; SCI, Spinal cord injury; SEM, Standard error of the mean; TBI, Traumatic brain injury; VaD, Vascular dementia

* Corresponding author at: Department of Chemical, Biological, Pharmaceutical and Environmental Sciences, University of Messina, Viale Ferdinando Stagno D'Alcontres n°31, 98166 Messina, Italy.
E-mail address: salvator@unime.it (S. Cuzzocrea).

https://doi.org/10.1016/j.nbd.2019.01.007
Received 3 September 2018; Received in revised form 12 December 2018; Accepted 15 January 2019
Available online 17 January 2019
0969-9961/

hyperhomocystinemia, hypertension, and hyperlipidemia (Craft, 2009; Purnell et al., 2009). VaD is frequently initiated by an acute, specific event such as transient ischemic attack or stroke in which blood flow to the brain has been stopped. It can also advance more gradually over time from very small obstructions or the slowing of blood flow. Instead of seeing VaD a clear result of neuronal death and the break of neuronal networks that maintenance cognitive function, VaD-brain malfunction is induced by vascular risk factors and hypoxia. The molecular links between stoke and VaD are presently not clearly comprehended. There are many demands raised in research connecting stroke and dementia, which are principally unanswered. Hence, it is essential to apprehend early events of stroke, and stroke leading to VaD. However, not all individuals who experience a stroke develop VaD (Siracusa et al., 2017). The majority of people affected by VaD have cognitive deficits, partly owing to the cerebral hypoperfusion-induced ischemia, oxidative stress, and neuroinflammation that are associated with the disease (Bar et al., 2003). Nuclear factor erythroid 2 related factor 2(Nrf2), a common transcription factor, is a principal cytoprotective defender against oxidative stress (Crunkhorn, 2012). Hitherto, the Nrf2 pathway has been recognized as a key factor in preventing oxidative injury in cerebral ischemia and dementia (Janda et al., 2015; Narayanan et al., 2015). Other studies reported that Nrf2 subdues inflammation by inhibiting nuclear factor (NF)-κB activation through control of the redox balance (Thimmulappa et al., 2006).

Despite the pressing need for strategies for the treatment of VaD, few currently exist (Toyama et al., 2014). The use of anti-inflammatory treatments for central nervous system (CNS) neuroinflammation has thus far proven clinically disappointing. For this reason, new therapeutic strategies are being considered. Some drugs may demonstrate their healing potential by regulating neuroinflammation, rather than by their habitually attributed actions only. ALIAmides are endogenous N-acylethanolamines (NAEs) whose levels are mostly normalized by enzymes involved in their degradation and synthesis (Esposito et al., 2014). Palmitoylethanolamide (PEA) is a prototype ALIAmide well-known for its analgesic, anti-inflammatory, and neuroprotective properties. PEA exerts its anti-inflammatory effects by down-regulating mast-cell (MC) degranulation via an autacoid local inflammation antagonism (ALIA) mechanism. In our studies, we proved the beneficial effects of PEA alone or associated with antioxidants in several experimental models of neuroinflammation, such as spinal cord injury (SCI), traumatic brain injury (TBI), and stroke (Ahmad et al., 2012a; Ahmad et al., 2012b; Paterniti et al., 2013).

The inhibition of PEA degradation by targeting NAE-hydrolyzing acid amidase (NAAA), its catabolic enzyme, represents an alternative strategy for treating neuroinflammation. Various NAAA inhibitors have been designated (Sasso et al., 2013; Saturnino et al., 2010; Solorzano et al., 2009), which modulate responses induced by inflammation (Li et al., 2012; Solorzano et al., 2009) and raise PEA levels in vitro (Favaloro et al., 2012; Solorzano et al., 2009). Surprisingly, pharmacological or genetic handling of PEA catabolism may cause important side effects (Benito et al., 2012; Hoyer et al., 2014; Rivera et al., 2015; Siegmund et al., 2013). Hence, it is essential to find a new approach to the inhibition of NAAA, with the use of molecules able to modulate NAAA activity, permitting a finer 'tuning' of PEA levels. Recent studies revealed that pharmacological modulation of NAAA can be done with the oxazoline contained in PEA (PEA-OXA) (Impellizzeri et al., 2016). The synthesis and biological plant sources of PEA-OXA were reported in a model of carrageenan-induced inflammation (Impellizzeri et al., 2016). In particular, Petrosino et al. and Impellizzeri et al. (Impellizzeri et al., 2016; Impellizzeri et al., 2017) showed that PEA-OXA exerts stronger anti-inflammatory and anti-nociceptive effects than PEA, at least in part through modulation of the NAAA. A previous study also confirmed the neuroprotective effects of PEA-OXA in animal models of neuroinflammation, such as traumatic brain and spinal cord injuries (Impellizzeri et al., 2017). Recently, Cordaro et al. also showed that PEA-OXA treatment reduced neurodegeneration and the neuroinflammatory response in an MPTP model of Parkinson's disorder by neutralizing excessive ROS and activating an intracellular antioxidant system (Cordaro et al., 2018). Hence, the aim of the present study was to better evaluate the anti-inflammatory and neuroprotective effects of PEA-OXA in a mouse model of VaD by repeated bilateral common carotid arteries occlusion.

2. Materials and methods

2.1. Animals

CD1 mice (male 25–30 g; Envigo, Milan, Italy) were housed in steel cages in a room at 22 ± 1 °C with a 12-h light, 12-h dark cycle, and furnished with regular rodent food and water. The University of Messina Review Board for the care of animals approved the research. All animal experiments observed the new regulations in Italy (D.Lgs 2014/26), as well as EU regulations (EU Directive 2010/63).

2.2. Animal model of VaD induction

VaD induction was performed in mice, as previously indicated (Siracusa et al., 2017; Wang, 2014). Briefly, after anesthesia, the bilateral carotid arteries were obstructed by ligation for 10 min, and then unrestricted for 10 min, and this cycle was repeated three times. The threading was removed and the incision closed. Fifteen days after induction, the mice were killed by decapitation, and their brains collected and processed.

2.3. Experimental groups

The animals were indiscriminately distributed into the following groups:

Group 1: Sham + vehicle = mice were exposed to the surgery without carotid arteries ligation and were treated orally with vehicle (carboxymethylcellulose 1% wt/vol in saline) once a day for 15 days ($N = 10$).

Group 2: Sham + PEA-OXA = same as the sham + vehicle group, but PEA-OXA (10 mg/kg orally, dissolved in carboxymethylcellulose 1% wt/vol in saline) was administered 24 h after the surgical procedure without carotid arteries ligation and once a day for 15 days thereafter (data not shown) (N = 10).

Group 3: VaD + vehicle = the mice were subjected to the VaD surgery described above and treated with vehicle as indicated for Sham + vehicle group (N = 10).

Group 4: VaD + PEA-OXA = same as the VaD + Veh group, but PEA-OXA (at a dose of 10 mg/kg orally, dissolved in carboxymethylcellulose 1% wt/vol in saline) was administered 24 h after the surgical procedure and once a day for 15 days thereafter (N = 10).

The dose and the route of administration of PEA-OXA were chosen based on a previous study (Cordaro et al., 2018). 5 mice for immunohistochemical analyses and 5 mice for western blot analyses for each experimental group) were used. Replicates for each experimental condition and histochemical staining were acquired from each mouse in each experimental group.

2.4. Behavioral testing

Behavioral testing on all mice was conducted one day before and 15 days after VaD induction.

2.5. Novel object recognition test (NOR)

This model was performed as previously described (Siracusa et al., 2017). The exploration time for the animal to investigate the new object was reported.

2.6. Morris water maze (MWM)

To examine spatial learning and memory, the MWM procedure was performed as described (Wang et al., 2015). The escape latency, the time it took the mice to find and stand on a platform under water, was evaluated in navigation trials (3 trials per day for 5 consecutive days), and the frequency time around and within the quadrant of the platform was measured in probe trial (at 6th day) (Xiong et al., 2017).

2.7. Light microscopy

Histopathological examination with hematoxylin and eosin staining was performed as previously described (Siracusa et al., 2017). The brains were quickly collected and fixed in 4% formalin. Following dehydration with ethanol and embedding with paraffin, 7 μm sections were prepared and stained. The hippocampal CA1 and CA3 areas were then observed by an optical microscope (Leica QWin V3, Cambridge, UK). Ischemic neuronal damage was scored on a gradation of 0 = normal, 1 = a few neurons damaged, 2 = many neurons damaged, and 3 = majority of neurons damaged (Fujii et al., 1997). All the histological studies were completed in a blinded fashion.

For Nissl staining, brain paraffin tissues were prepared with a 20 μm thickness. The sections were submersed in 0.2% Cresyl violet for 5 min and then enclosed with xylene-based mounting medium.

In every slice (three slices per mouse), we counted the number of surviving intact neuronal cells per mm length of hippocampal CA1 and CA2/3 subfield in both hemispheres (Zhen et al., 2014). Sections were observed blinded by a second investigator using a light microscope (Leica QWin V3, Cambridge, UK).

2.8. Immunohistochemical localization of Nrf2 and iNOS

The immunohistochemical techniques used have been previously described (Siracusa et al., 2017). Slices were incubated overnight with one of the following primary antibodies (specific for each, whether polyclonal or monoclonal): anti-Nrf-2 (Santa Cruz Biotechnology (SCBT), 1:250 in PBS, v/v), or anti-iNOS (SCBT, 1:250 in PBS, v/v). Sections were cleaned with PBS and incubated with peroxidase-conjugated bovine anti-mouse immunoglobulin G (IgG) secondary antibody or peroxidase-conjugated goat anti-rabbit IgG (Jackson Immuno Research, West Grove, PA, USA, 1:2000). Specific labeling was detected with a biotin-conjugated goat anti-rabbit IgG or biotin-conjugated goat anti-mouse IgG and avidin-biotin peroxidase complex (Vector Laboratories, Burlingame, CA, USA). The counter-stain was developed with diaminobenzidine (DAB; brown color) and nuclear fast red (red background). To verify antibody-binding specificity, control slices were incubated with only the primary antibody or the secondary antibody, neither of which gave positive staining. Images were collected using a Zeiss microscope and Axio Vision software. Images were captured with 20× objective lenses (Varghese et al., 2014), using a Zeiss microscope (Zeiss, Germany) equipped with an AxioCam MRc5 camera (Zeiss, Germany).

The digital images were opened in ImageJ, followed by deconvolution using the color deconvolution plug-in. When the IHC profiler plug-in is selected, it automatically plots a histogram profile of the deconvoluted DAB image, and a corresponding scoring log is displayed (Sawant et al., 2016). The histogram profile corresponds to the positive pixel intensity value obtained from the computer program (Varghese et al., 2014). All immunohistochemical analyses were carried out by two observers blinded to the treatment.

2.9. Immunofluorescence of MAP-2, GFAP, and Iba-1

After deparaffinization and rehydration, detection of MAP-2, GFAP, and Iba-1 was carried out as previously indicated (Siracusa et al., 2017). Sections were incubated with monoclonal anti-MAP-2 (Millipore; 1:100 in PBS, v/v), monoclonal anti-GFAP (SCBT; 1:200 in PBS, v/v), or monoclonal anti-Iba-1 (SCBT; 1:200 in PBS, v/v), antibodies in a humidified chamber overnight at 37 °C. Sections were seen and photographed by a Leica DM2000 microscope (Leica, Milan, Italy). Digital images were collected and figure montages arranged using Adobe Photoshop CS6 (Adobe Systems, Milan, Italy).

2.10. TUNEL staining

TUNEL staining was performed according to a Roche protocol (Cordaro et al., 2017).

2.11. Analysis by LC-APCI-MS of PEA levels

Liquid chromatography-atmospheric pressure chemical ionization-mass spectrometry (LC-APCI-MS) analyses of PEA levels were carried out as previously described (Bisogno et al., 1997; Marsicano et al., 2002). Briefly, brains were homogenized in a solution of chloroform/methanol/Tris-HCl 50 mM pH 7.4 (2:1:1 by vol.) containing 5 pmol of $[^2H]_4$-PEA as internal deuterated standard. The lipid-containing organic phase was pre-purified by open-bed chromatography on silica gel, and fractions obtained by eluting the column with a solution of chloroform/methanol (90:10 by vol.) were analyzed by LC-APCI-MS by using a Shimadzu HPLC apparatus (LC-10ADVP) coupled to a Shimadzu (LCMS-2020) quadrupole MS via a Shimadzu APCI interface. LC-APCI-MS analyses of PEA were carried out in the selected ion monitoring (SIM) mode, using m/z values of molecular ions +1 for deuterated and undeuterated compound, respectively of 304 and 300. PEA levels were calculated on the basis of their area ratio with the internal deuterated standard signal areas, and their amounts (pmol) were normalized per g of brain.

2.12. Western blots for IKB-α, nuclear factor-κB (NF-κB) p65, COX-2, iNOS, NRF-2, HO-1, MnSOD, MAP-2, IL-10, BAX, BCL-2, NAAA and FAAH

Cytosolic and nuclear extracts were prepared as previously described on hippocampus tissues (Esposito et al., 2016). The following primary antibodies were used: anti-IκB-α (SCBT, DBA Italia srl, Milan, Italy; 1:500), anti-NF-κB p65 (SCBT; 1:500), anti-COX-2 (SCBT; 1:500), anti-iNOS (BD Transduction Laboratories, 1:500), anti-BAX (SCBT; 1:500), anti-Bcl-2 (SCBT; 1:500), anti-IL-10 (SCBT; 1:500), anti-MAP-2 (Millipore; 1:500), anti-Nrf-2 (SCBT; 1:500), anti-HO-1 (SCBT; 1:500), anti-MnSOD (Millipore; 1:500), and anti-NAAA (Millipore; 1:500), anti-FAAH (Abnova; 1:500) in 1× phosphate-buffered saline, 5% w/v non-fat dried milk, 0.1% Tween-20 at 4 °C overnight. Membranes were incubated with peroxidase-conjugated bovine anti-mouse IgG secondary antibody or peroxidase-conjugated goat anti-rabbit IgG (Jackson ImmunoResearch, West Grove, PA, USA; 1:2000) for 1 h at room temperature. To establish that blots were loaded with identical volumes of lysate, they were also probed with anti-β-actin or anti-lamin A/C antibodies. Relative expression of protein bands was detected with a chemiluminescence detection system reagent, according to the manufacturer's instructions (Super Signal West Pico Chemiluminescent Substrate; Pierce). Relative expression of protein bands was calculated by densitometry with BIORAD ChemiDoc™ XRS + software and standardized to β-actin or lamin A/C levels. Images of blot signals (8 bit/600 dpi resolution) were imported to analysis software (Image Quant TL, v2003).

2.13. Materials

All compounds were acquired from Sigma-Aldrich, while PEA-OXA was a kind gift from Epitech Group Spa (Saccolongo, Italy). Deuterated standard - $[^2H]_4$-PEA - was purchased from Cayman Chemical (Cabru, Arcore, Italy).

All other substances were of the uppermost profitable grade available. All stock solutions were prepared in non-pyrogenic saline (0.9% NaCl; Baxter, Milan, Italy) or 10% dimethyl sulfoxide.

2.14. Statistical evaluation

All values in the images and text are expressed as mean ± standard error of the mean (SEM) of N observations. For in vivo studies, N represents the number of animals. In experiments involving histology and immunohistochemistry, the illustrations represent the outcomes of at least three independent experiments. A p-value of < 0.05 was considered significant. The results were analyzed by one- or two-way ANOVA, followed by a Bonferroni post-hoc test for multiple comparisons.

For PEA levels analysis, data were analyzed by using GraphPad Prism 7 (GraphPad Software, Inc., La Jolla, CA, USA), and one-way analysis of variance (ANOVA) followed by Newman-Keuls multiple comparison test was used for analysis.

3. Results

3.1. Effects of PEA-OXA on NAAA and FAAH modulation and endogenous PEA levels after VaD induction

Previous work reported that PEA-OXA could exert its anti-inflammatory action at least in part by NAAA modulation (Petrosino et al., 2017). With this in mind, western blot analysis for NAAA expression was conducted. Basal levels of NAAA were observed in the sham groups. By contrast, increased levels of NAAA were found in VaD-subjected animals compared to the sham animals. PEA-OXA treatment was able to reduce NAAA levels (Fig. 1 A). Accordingly, we also demonstrated that the endogenous levels of PEA were strongly decreased in the brains of mice after VaD induction (Fig. 1 B), and PEA-OXA treatment significantly increased the levels of the endogenous PEA in the brains of mice with VaD (Fig. 1 B).

In addition, western blot for FAAH expression was conducted. Basal levels of FAAH were found in sham animals. Increased levels of FAAH were observed in VaD-subjected mice compared to the sham (Fig. 1 C). PEA-OXA was not able to reduce in a significant way FAAH expression compared to vehicle group (Fig. 1 C).

3.2. Effect of PEA-OXA on histological parameters and neuronal death

To assess the gravity of damage in the hippocampal regions 15 days after injury, all sections were stained with H&E. Control mice showed a regular architecture in the hippocampus. Nerve cells were abundant, strictly organized, and had round nuclei (Fig. 2 A; for hippocampal CA1 and CA3 regions see magnification higher A1, A2, and relative histological analysis D). A low number of disordered and severely stained nerve cells was observed in the hippocampal areas of mice subjected to VaD injury (Fig. 2 B, for hippocampal CA1 and CA3 regions see magnification higher B1, B2 and relative histological analysis D). In contrast, brain sections from VaD mice treated with PEA-OXA exhibited an evident reorganization of hippocampal CA1 and CA3 regions, with an increased number of hippocampal neurons (Fig. 2 C, for hippocampal CA1 and CA3 regions see magnification higher C1, C2 and relative histological analysis D).

In addition, to evaluate the effect of PEA-OXA on cerebral ischemic injury by VaD induction, we used Nissl staining to detect neuron cell death in this model. The sham subjects did not exhibit dead cells in CA1 and CA3 (Fig. 3 A; see A1, A2, A3, and graphs D, E). Increased neuronal dead cells were observed in both CA1 and CA3 regions in the VaD vehicle groups (Fig. 3 B, see B1, B2, B3 and D, E). PEA-OXA reversed the presence of injured neuron cells in the CA1 and CA3 regions of the hippocampus after VaD induction (Fig. 3 C, see C1, C2, C3 and graphs D, E).

3.3. Effects of PEA-OXA on apoptosis

Apoptosis has been proposed to justify the cell loss seen in numerous neurological disorders, including Alzheimer's disease and VaD (Favaloro et al., 2012).

Reactive oxygen species (ROS) and the resulting oxidative stress play a critical role in apoptosis. Given this, we also evaluated the effect of PEA-OXA on the apoptotic process. The TUNEL assay was used. TUNEL staining showed that there were more apoptotic cells in the brain tissues of VaD-subjected mice (Fig. 4 B, B1 for CA1 region, B2, B3 for CA3 region, and see D) than in sham groups (Fig. 4 A, A1 for CA1 region, A2, A3 for CA3 region, and see D). PEA-OXA treatment significantly reduced the number of apoptotic cells (Fig. 4 C, C1 for CA1 region, C2, C3 for CA3 region and see D). At the same time, the expression of proapoptotic protein such as BAX and anti-apoptotic protein such as Bcl-2 was detected by western blot. Low levels of BAX and high levels of Bcl-2 were found in the sham groups (Fig. 4, E, F). Moreover, increased levels of BAX and reduced levels of Bcl-2 were found in VaD-subjected animals than in the controls (Fig. 4, E, F). PEA-OXA was able to reverse these levels (Fig. 4 E, F).

3.4. Effects of PEA-OXA on astrocytes, microglia, and neuronal cells

To evaluate the effect of PEA-OXA on neuroinflammation induced by VaD induction, we examined astrocytes (GFAP), microglia (Iba-1), and neuronal cell (MAP-2) markers by immunofluorescence staining. Increased positive stainings for GFAP and Iba-1 were observed in VaD vehicle animals compared to the sham animals (Fig. 5 A, B and see particle A1, B1 Fig. 5 D, E and see particle D1, E1). PEA-OXA treatment was able to reduce immunoreactivity for GFAP and Iba-1 (Fig. 5 C, F and see particles C1, F1). In addition, reduced positive staining for MAP-2 was observed in VaD animals compared to sham, while PEA-OXA counteracted this reduction (Fig. 6 A, B, C, A1, A2, A3, B1, B2, B3, C1, C2, C3). Western blot analysis of MAP-2 also showed a reduced expression in VaD-subjected animals compared to sham (Fig. 6 D). PEA-OXA significantly increased MAP-2 expression (Fig. 6 D).

3.5. Effects of PEA-OXA on the NF-κB pathway

To study the possible mechanisms of PEA-OXA anti-inflammatory effects, we evaluated the NF-κB pathway by western blot. In the sham group, NF-κB was steadied by IκB in the cytoplasm. After VaD induction, it initiated the degradation of IκB-α to permit NF-κB transportation into the nucleus. Our results showed that, following injury, the level of IκB-α protein was diminished in the cytoplasm (Fig. 7 A), while high levels of NF-κB p65 were seen in the nucleus compared to the sham group (Fig. 7 B). However, PEA-OXA treatment appreciably prevented the degradation of IκB-α and the nuclear NF-κB translocation compared to the VaD + vehicle group (Fig. 7 A, B). In addition, iNOS and COX-2 expressions were evaluated using western blot analysis. A significant increase in iNOS and COX-2 expression was observed in brains from mice subjected to VaD compared to controls (Fig. 7C, D), while a significant decrease in iNOS and COX-2 expression was observed after PEA-OXA treatment (Fig. 7 C, D).

Immunohistochemical analysis also showed important positive staining for iNOS in VaD + vehicle mice compared to controls (Fig. 8 A, A1, B, B1 and see D, E). PEA-OXA treatment reduced iNOS positive staining compared to VaD + vehicle mice (Fig. 8 C, C1 and see D, E).

In addition, many of the proinflammatory cytokines shown to be suppressed by IL-10 are known to be regulated by the transcription factor NF-κB (Driessler et al., 2004). However, IL-10, an anti-inflammatory mediator, has been identified as one of the main cytokines associated with the incidence of dementia (Magalhaes et al., 2017). Reduced levels of IL-10 were found in VaD + vehicle mice compared to controls (Fig. 7 E), while PEA-OXA treatment was also able to increase these anti-inflammatory cytokine levels (Fig. 7 E).

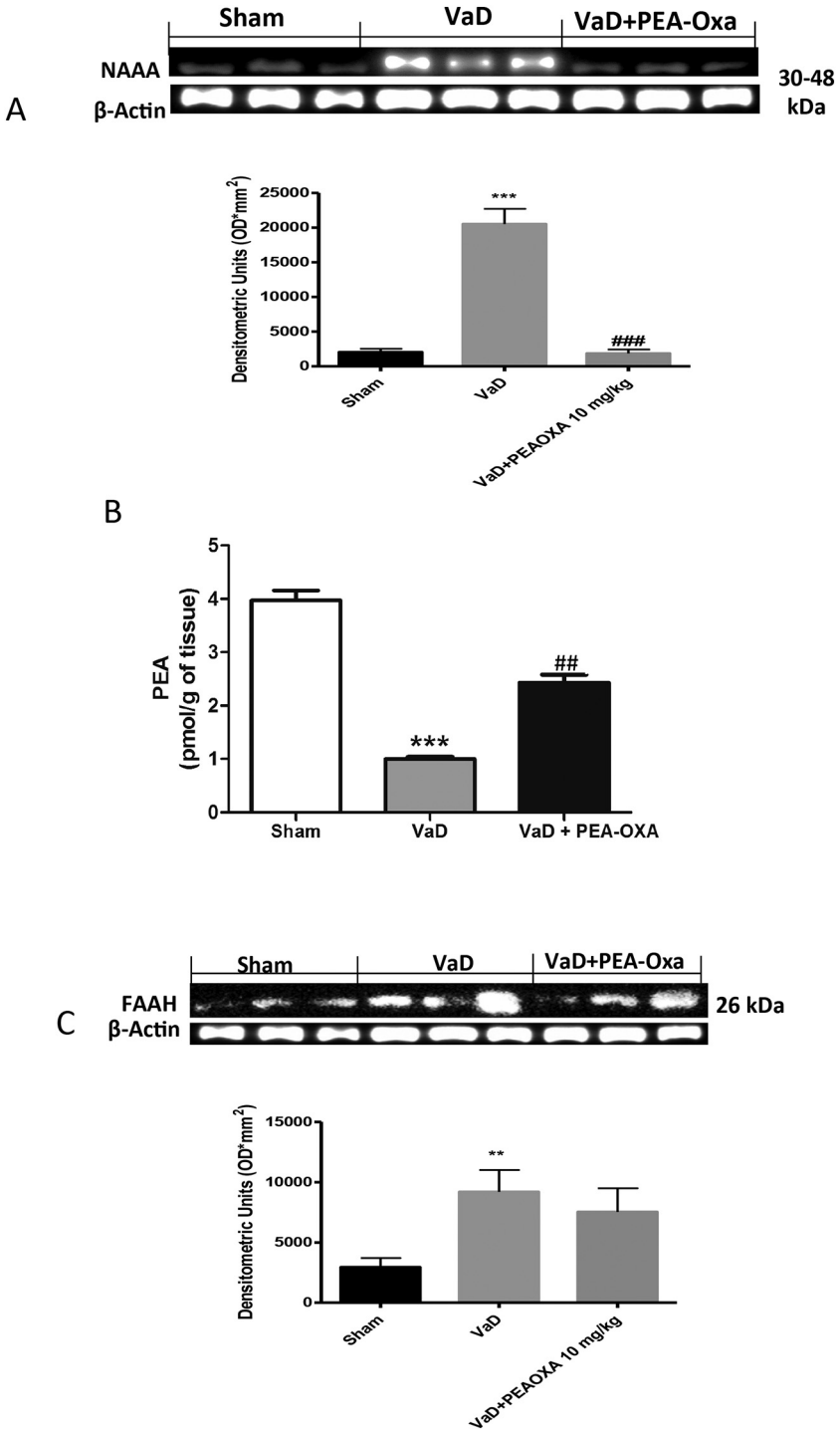

Fig. 1. PEA-OXA treatment on NAAA and FAAH modulation and endogenous brain PEA levels.
Demonstrative western blot on hippocampus tissues showed the effects of PEA-OXA on NAAA modulation. Oral administration of PEA-OXA significantly reduces NAAA expression (A) as well as not significantly reduces FAAH expression (B). Figure (C) showed endogenous levels of PEA in the brains of mice after induction of VaD and treatment with PEA-OXA. Indicated is a representative blot of lysates (5 animals/group) with a densitometric analysis for all. The results are expressed as means ± SEM of 5 animals for each group. $^{***}P < 0.001$ vs. sham; $^{\#\#}P < 0.01$ vs VaD, $^{\#\#\#}P < 0.001$ vs. VaD.

3.6. Effects of PEA-OXA on the Nrf-2 pathway

Nrf-2 controls the expression of several antioxidant genes such as Mn-SOD and HO-1 and plays a crucial role in cellular defense against oxidative stress (Todorovic et al., 2016). Thus, we performed western blot analysis to determine whether PEA-OXA could also modulate the Nrf2-mediated antioxidant response. A basal expression of Nrf-2, Mn-SOD, and HO-1 was observed in the sham groups (Fig. 7 F, G, H). By contrast, VaD induction provoked the activation of antioxidant systems of Nrf-2, Mn-SOD, and HO-1 compared to the sham groups (Fig. 7 F, G, H). PEA-OXA treatment was able to upregulate this antioxidant response (Fig. 7 F, G, H).

The data on the Nrf-2 pathway were also confirmed by immunohistochemistry. PEA-OXA administration increased the positive staining for Nrf-2 compared to the vehicle groups (Fig. 9 A, B, C, A1,B1,C1 and see graphs D, E).

3.7. Effect of PEA-OXA on memory deficits

We used the Novel object recognition test (NOR) test to evaluate changes in cognitive function. During training, controls and VaD animals presented no significant difference in their exploration time of novel objects. At 15 days following injury, the VaD animals showed meaningfully reduced interest in the novel object (Fig. 10 A), denoting

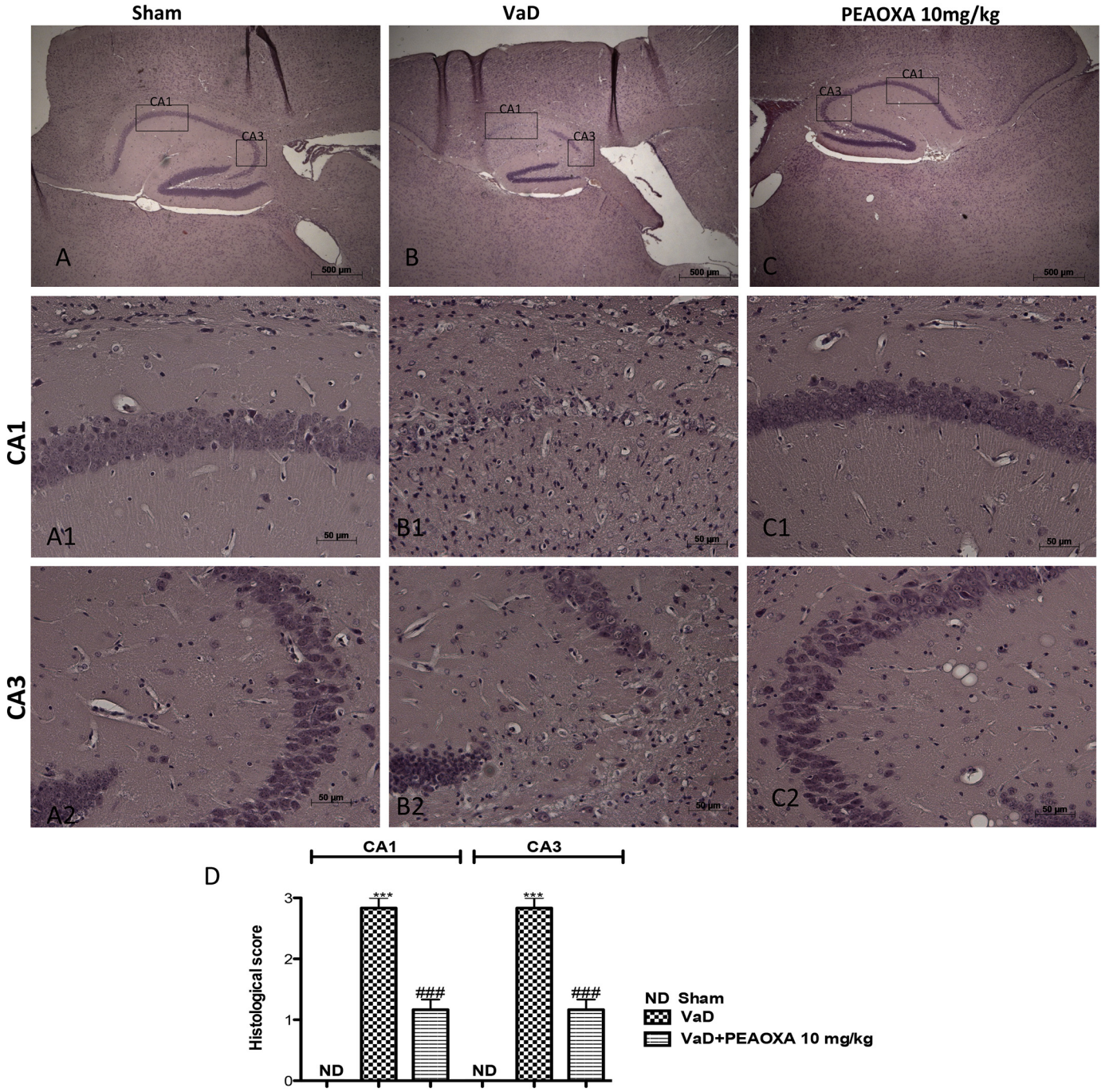

Fig. 2. PEA-OXA treatment on VaD induced histological damage.
Histological evaluation in CA1 and CA3 regions respectively (hematoxylin/eosin staining): (A, A1, A2) sham group, (B, B1, B2) VaD + vehicle group, (C, C1, C2) VaD + PEA-OXA group, (D) histological score, Figures are expressive of at least three separated experiments. Values are means ± SEM of 5 animals for each group; ***P < 0.001 vs sham, $^{###}$P < 0.001 vs VaD. ND: not detectable.

an alteration of cognitive function; while the exploration time for novel object recognition was increased in mice treated with PEA-OXA compared to the vehicle groups (Fig. 10 A).

The Morris water maze (MWM) test was performed to evaluate the effect of PEA-OXA on memory impairments. The time taken to find the platform during training was increased in VaD-subjected animals compared to the controls (Fig. 10 B). The treatment with PEA-OXA reduced this escape latency (Fig. 10 B). In addition, the frequency time around and within the target quadrant of the platform during probe trial was reduced in VaD + vehicle animals (Fig. 10 C). PEA-OXA treatment increased the frequency time, ameliorating the cognitive deficits (Fig. 10 C).

4. Discussion

VaD is a common type of dementia in older people, characterized by gradually worsening memory and other cognitive actions resulting from chronic reduced blood flow in the brain (Sekhon et al., 1997). VaD is a clinical mental condition, caused by cardiovascular pathological modifications and cerebrovascular disease, which can determine ischemic or hemorrhagic brain tissue lesions (Roman, 2002; Seitz et al., 2011). The increased incidence of VaD imposes a heavy economic and social

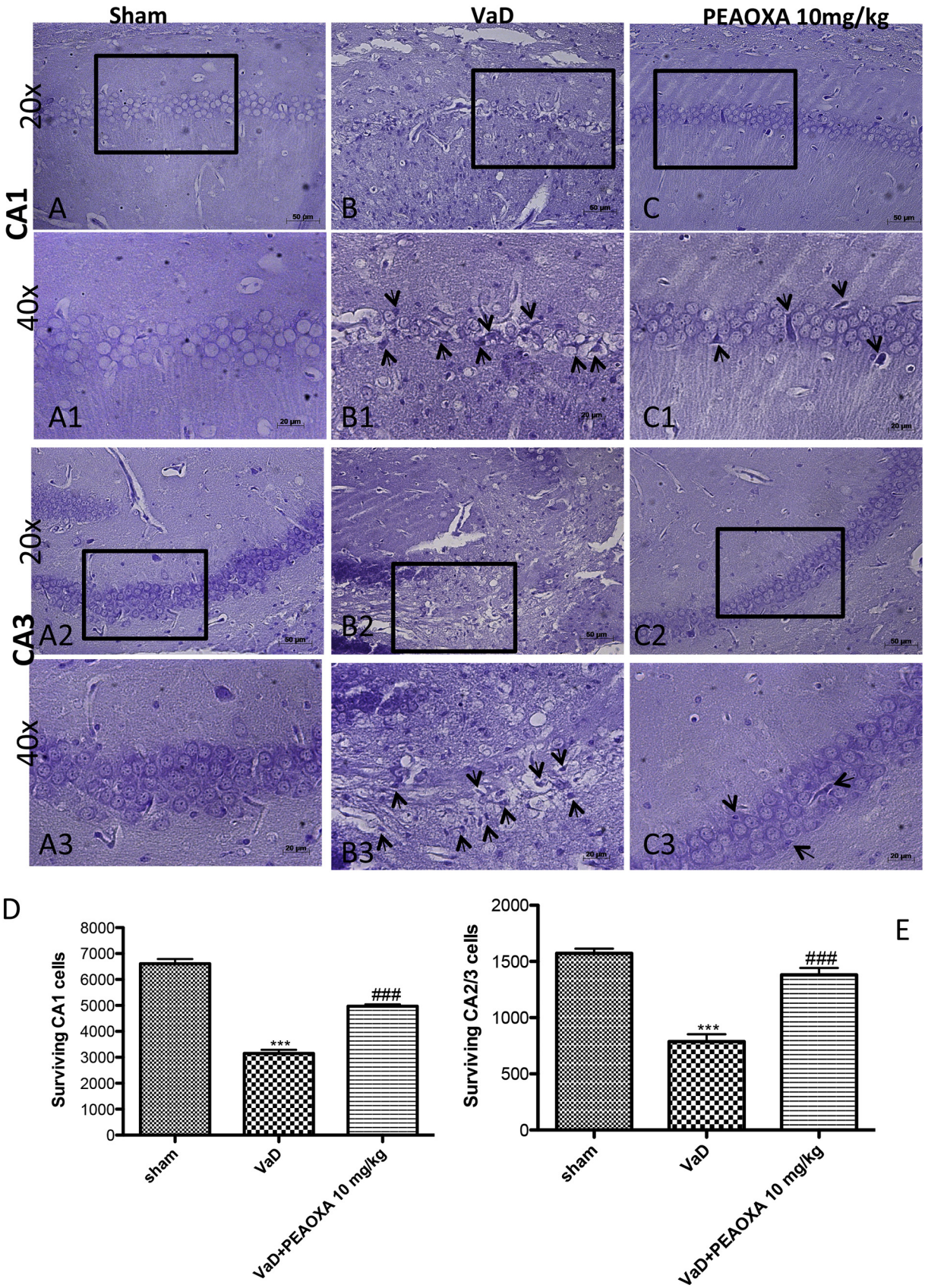

Fig. 3. PEA-OXA treatment on VaD induced neuronal death.
Neuronal death evaluation in CA1 and CA3 regions respectively (Nissle staining): (A, A1, A2 A3) sham group, (B, B1, B2, B3) VaD + vehicle group, (C, C1, C2, C3) VaD + PEA-OXA group, (D, E) number of surviving intact neuronal cells per mm length of hippocampal regions. Figures are representative of at least three separated experiments. 20× and 40× magnification are showed. Black arrows indicate stained positive cells (dead cells). Values are means ± SEM of 5 animals for each group; ***P < 0.001 vs sham, $^{###}$P < 0.001 vs VaD.

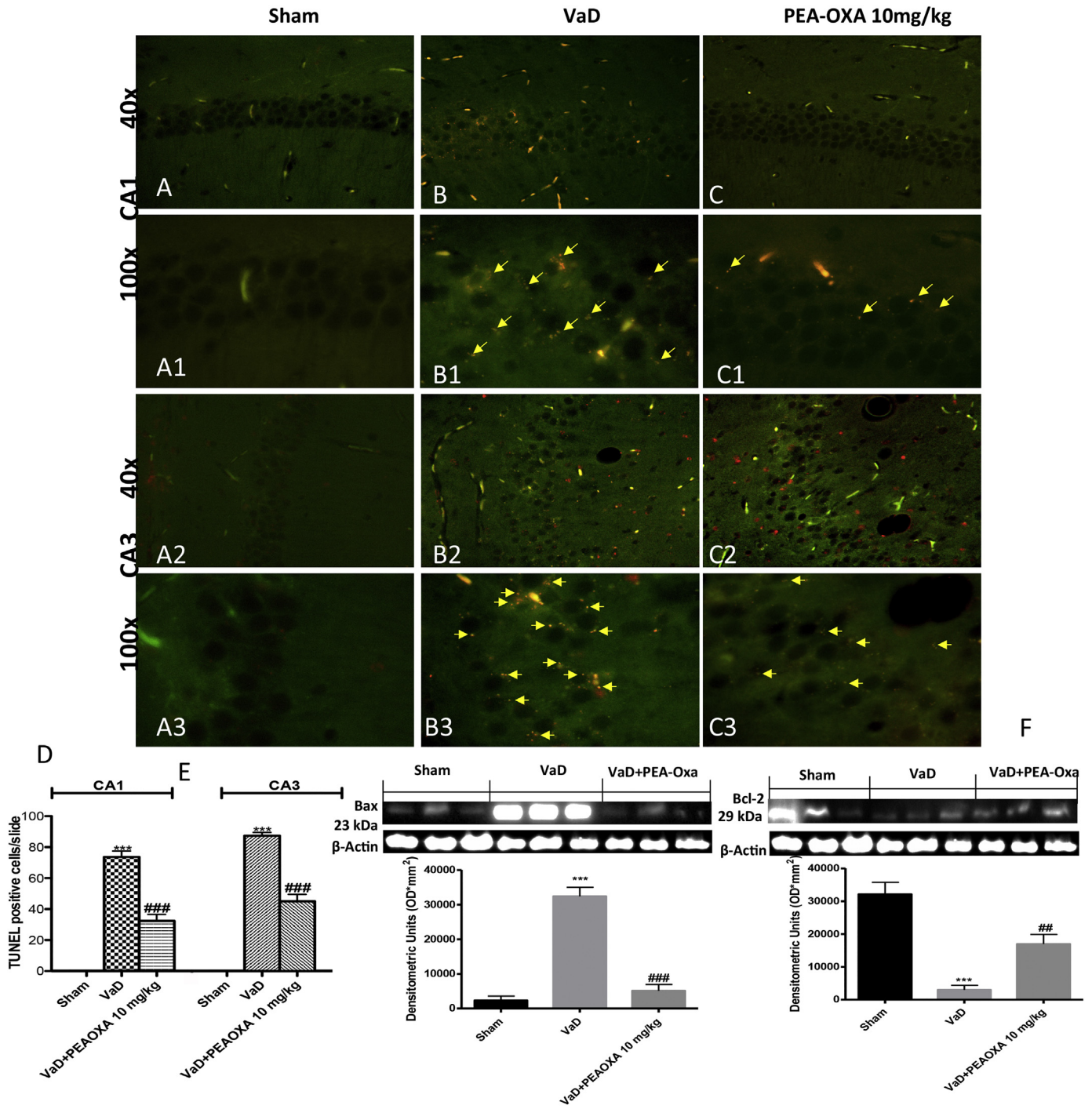

Fig. 4. PEA-OXA treatment on VaD induced apoptosis.
Tunel staining to identify positive apoptotic cells (yellow arrows) was performed. Sham (A, A1,A2,A3), VaD + vehicle (B, B1, B2, B3), VaD + PEA-OXA (C, C1, C2, C3), The number of apoptotic cells in CA1 and CA3 subfields of hyppocampus was scored (D). 40× and 100× magnification are showed. Images are representative of at least three experiments performed on different days. In addition, western blot analysis demonstrated Bax and Bcl-2 expression after VaD induction (E,F). Shown is a representative blot of lysates (5 animals/group) with a densitometric analysis for all animals. The results are expressed as means ± SEM of 5 animals for each group. $^{***}P < 0.001$ vs. sham; $^{\#\#}P < 0.01$ vs. VaD, $^{\#\#\#}P < 0.001$ vs. VaD.

burden on individuals, families, communities, and countries. To date, the accurate pathogenesis of VaD remains undefined and there is no successful treatment for VaD, although it is urgently needed (Ma et al., 2017).

Neuroinflammation plays a primary role in the pathophysiology of VaD and other SNC disorders. Stress, tissue damage, and associated inflammatory events may elicit an endogenous program that involves the production of lipid mediators able to stop inflammation and reinstate a homeostatic balance (Buckley et al., 2013; Piomelli and Sasso, 2014). Many molecules have been recognized in these protective mechanisms. Among these, the ALIAmide PEA, a member of the NAE family, a class of naturally lipid signaling molecules, has been found to exhibit beneficial effects alone and in combination in different models of inflammation, neuroinflammation, and pain (Impellizzeri et al., 2014; Paterniti et al., 2013). Recent studies have reported work with the anti-neuroinflammatory and neuroprotective actions of PEA

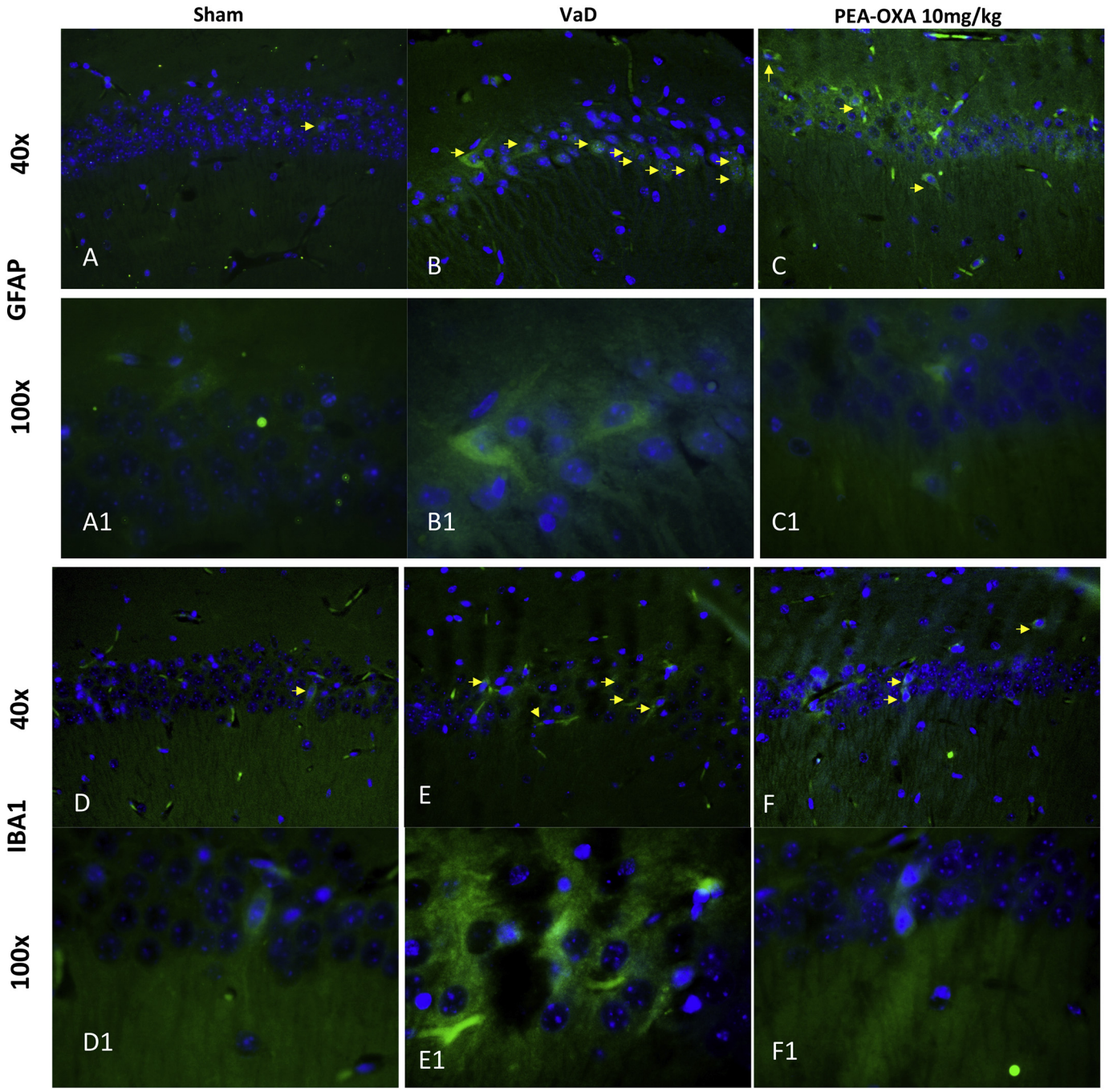

Fig. 5. PEA-OXA treatment on VaD induced astrocytes and microglia activation.
Immunofluorescence for GFAP (green) (see yellow arrows) and Iba-1 (green) (see yellow arrows) expression in hyppocampus respectively in sham animals (A, A1 and D,D1), VaD subjected animals (B, B1 and E, E1) and VaD-subjected animals treated with PEA-OXA (C, C1 and F, F1). Data are representative of at least three separated experiments. Images are representative of all animals in each group. All images were digitalized at a resolution of 8 bits into an array of 2048 × 2048 pixels. Pictures were captured at 40× and 100× magnification. Values are means ± SEM of 5 animals for each group.

(Alhouayek and Muccioli, 2014; Esposito et al., 2014; Fidaleo et al., 2014; Mattace Raso et al., 2014). In addition, the modulation of inflammatory responses can be achieved by increasing endogenous PEA levels by inhibiting its degradation or targeting FAAH (Ueda et al., 2010) and in particular its principal catabolic enzyme, NAAA (Ribeiro et al., 2015; Solorzano et al., 2009; Ueda et al., 2010; Yamano et al., 2012; Yang et al., 2015).

Pharmacological or genetic manipulation of PEA catabolism may sometimes lead to undesirable effects (Benito et al., 2012; Hoyer et al., 2014; Rivera et al., 2015; Siegmund et al., 2013). For this reason, it has been advised that pharmacologically modulating—and not blocking—the specific amidases such as NAAA could be essential to preserve the function of PEA in supporting cellular homeostasis, thanks to its quick on-demand synthesis and fast degradation (Skaper et al., 2015). Recent studies have explained the NAAA pharmacological modulation with the oxazoline of PEA (2-pentadecyl-2-oxazoline or PEA-OXA) (Impellizzeri et al., 2016). PEA-OXA, which is present in nature, can be speedily converted through exclusively physiological processes into PEA. The oxazoline (but not the equivalent non-cyclic structure PEA) is a weak inhibitor of NAAA compared to other known blockers. It was established that in the rat paw carrageenan (CAR) model, PEA-OXA had a superior beneficial effect compared to PEA

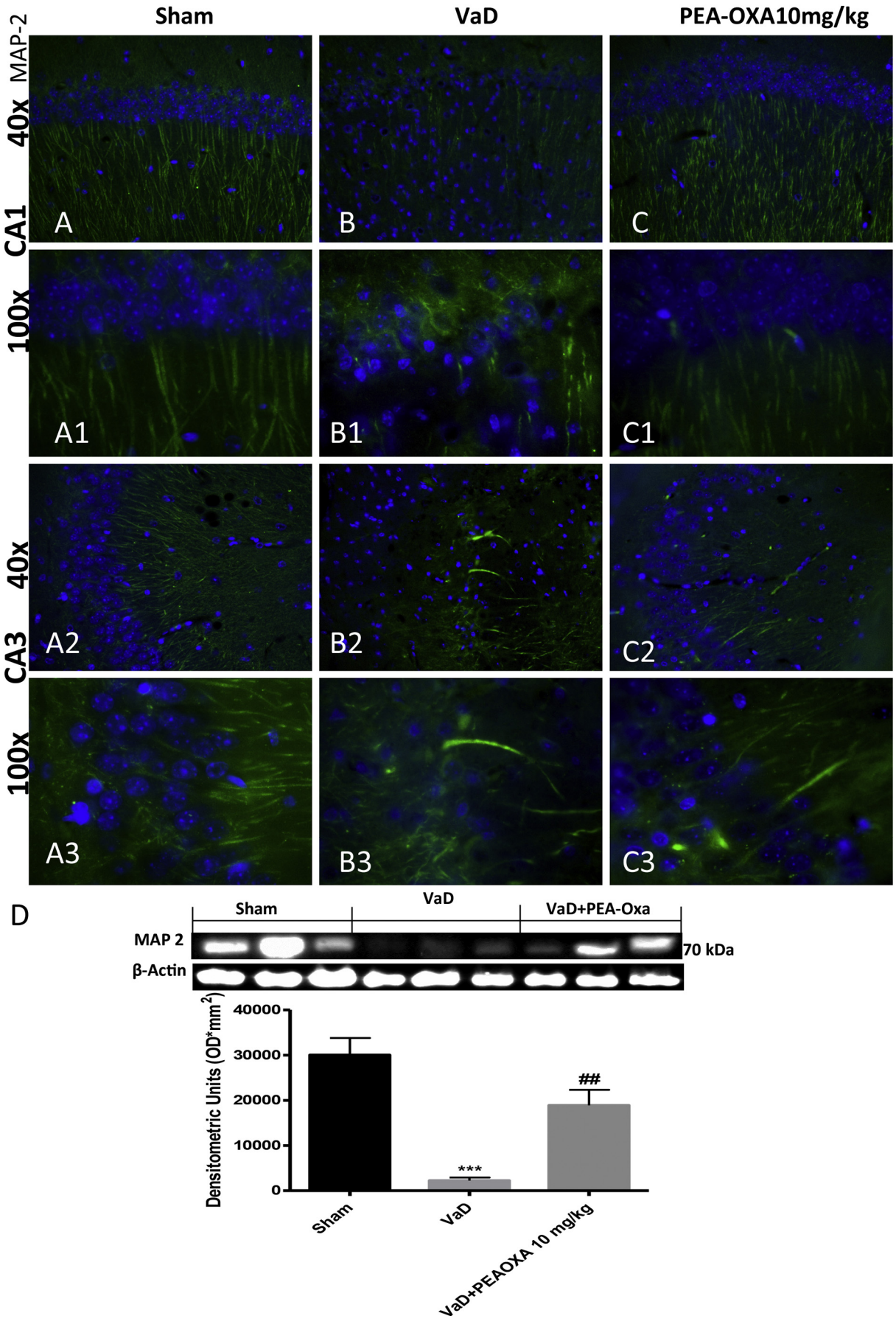

(caption on next page)

Fig. 6. PEA-OXA treatment on VaD induced loss of neuronal cells.
Immunofluorescence for MAP-2 (green) expression in CA1 and CA3 regions respectively in sham animals (A, A1,A2, A3), VaD subjected animals (B, B1, B2, B3) and VaD-subjected animals treated with PEA-OXA (C, C1, C2, C3). Data are representative of at least three separated experiments. Images are representative of all animals in each group. All images were digitalized at a resolution of 8 bits into an array of 2048 × 2048 pixels. Pictures were captured at 40× and 100× magnification. In addition, Western blot analysis demonstrated MAP-2 expression after VaD induction (D). Shown is a representative blot of lysates (5 animals/group) with a densitometric analysis for all animals. Values are means ± SEM of 5 animals for each group. $^{***}P < 0.001$ vs. sham; $^{\#\#}P < 0.01$ vs. VaD.

(Impellizzeri et al., 2016). The protective effect of PEA-OXA was also shown in other experimental models, such as SCI, TBI (Impellizzeri et al., 2017), and recently Parkinson's disease (Cordaro et al., 2018).

In the present study, we examined the anti-inflammatory and antioxidant effects of PEA-OXA in a mouse model of vascular dementia. We found that VaD caused important brain damage and neuronal death in the CA1 and CA3 regions of hippocampus. PEA-OXA treatment was able to reduce histological alterations (H&E staining) and neuronal death (Nissl staining) and ameliorate behavioral deficits associated with memory loss. This is in agreement with our previous studies, in which PEA-OXA reduced histological damage with neutrophil infiltration and behavioral deficits (Impellizzeri et al., 2017). Thus, the purpose of our research was to investigate the potential mechanisms through which PEA-OXA could reduce neuroinflammation and ameliorate memory deficits in VaD.

Recently, Petrosino et al. demonstrated that PEA-OXA is a modulator of NAAA activity and is able to increase the tissue levels of PEA in a model of CAR-induced paw edema (Petrosino et al., 2017). Interestedly, oxazoline derivatives of fatty acids have never been valued for their capability to inhibit FAAH and/or NAAA or for their potential inhibitory activity of inflammatory processes (Petrosino et al., 2017). Here, western blot analysis showed an increased expression of NAAA in VaD-subjected mice that was reduced by PEA-OXA treatment. On the contrary, PEA-OXA treatment was not able to significantly reduced FAAH expression compared to vehicle group. Anyway, accordingly with the modulation of NAAA expression, increased brain endogenous PEA levels were observed in VaD mice treated with PEA-OXA.

Microglia, a main type of immune cell in the brain, play a dominant

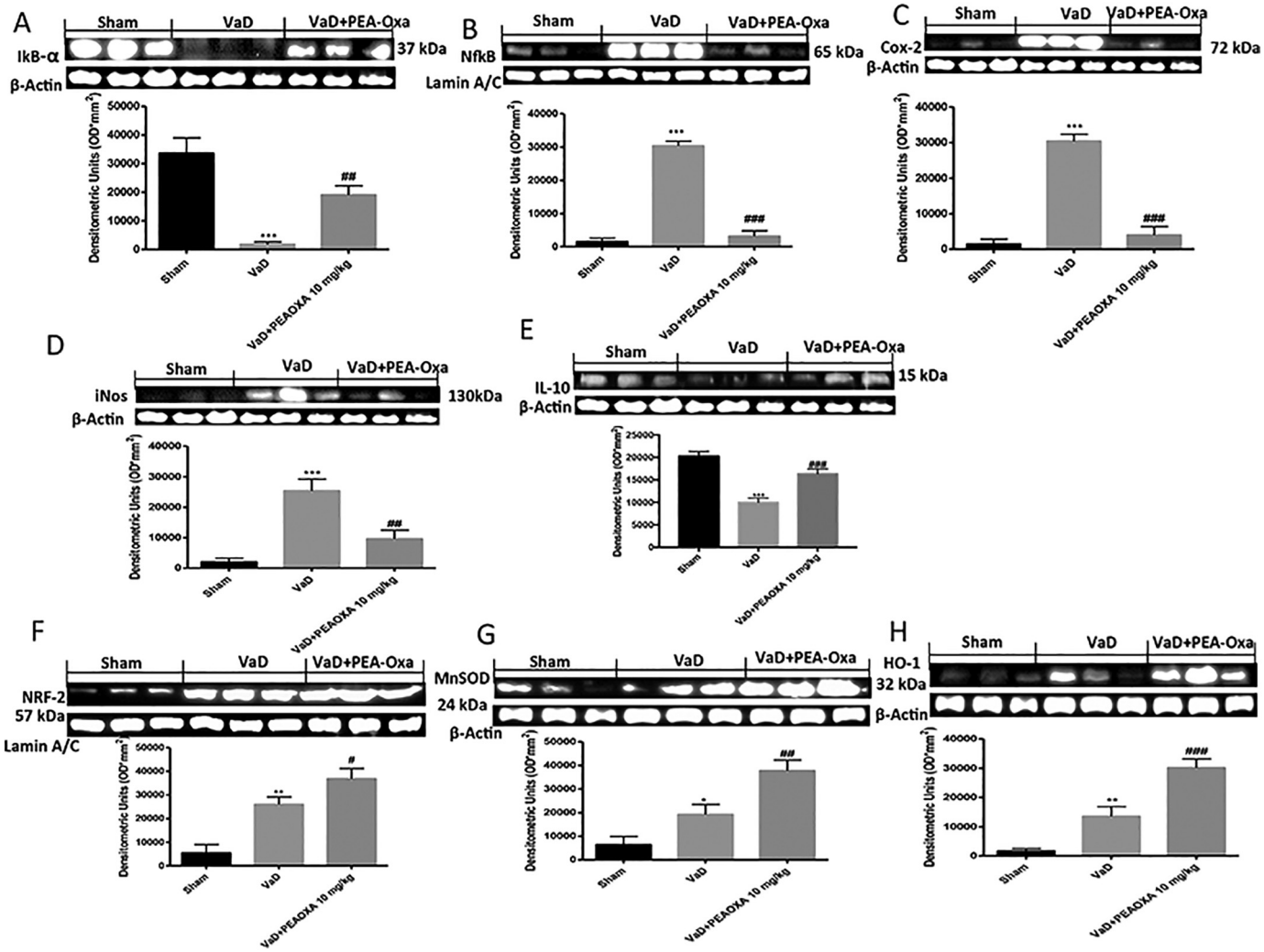

Fig. 7. PEA-OXA treatment on NF-κB inflammatory pathway and on NRF-2 antioxidant pathway after VaD induction.
Representative western blots on hippocampus tissues showed the effects of PEA-OXA on: (A) IκB-α degradation, (B) NF-κB p65 translocation, (C) COX-2 expression, (D) iNOS expression, (E) IL-10 expression, (F) NRF-2 expression, (G) MnSOD expression and (H) HO-1 expression after VaD induction. Shown is a representative blot of lysates from 5 animals/group, together with a densitometric analysis for all animals. The results in A, B C, D, E, F, G and H are expressed as means ± SEM of 5 animals for each group. $^{***}P < 0.001$ vs. sham; $^{\#\#}P < 0.01$ vs. VaD, $^{\#\#\#}P < 0.001$ vs. VaD; $^{*}P < 0.05$ vs. sham $^{**}P < 0.01$ vs. sham $^{\#}P < 0.05$ vs. VaD $^{\#\#}P < 0.01$ vs. VaD, $^{\#\#\#}P < 0.001$ vs. VaD.

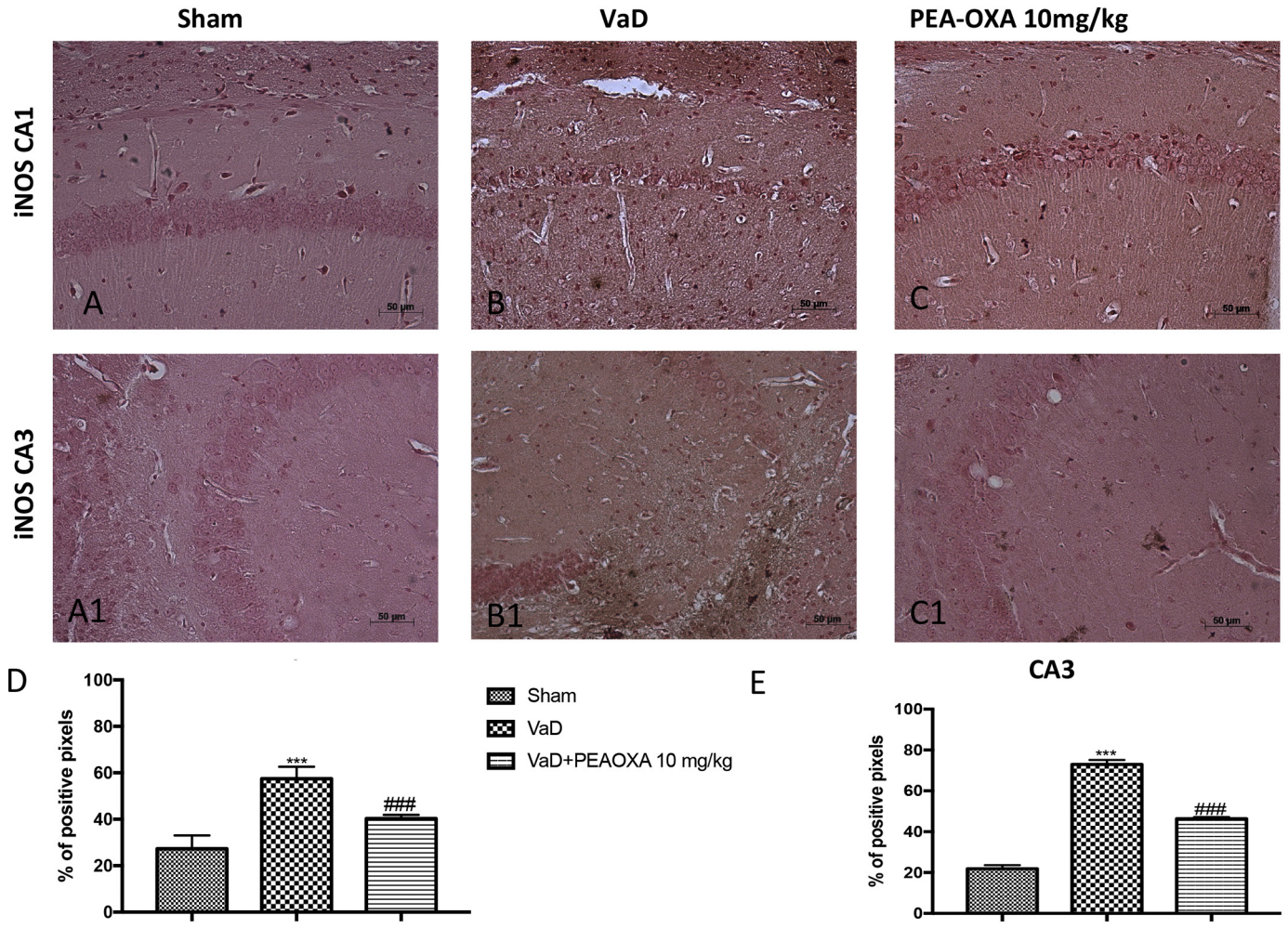

Fig. 8. Imunohistochemistry for iNOS after VaD induction.
Immunohistochemistry for iNOS in CA1 and CA3 regions respectively (A, A1) sham group, (B, B1) VaD + vehicle group, (C, C1) VaD + PEA-OXA group. The results are expressed as % of positive cells (D). Figures are representative of at least three independent experiments. Values are means ± SEM of 5 animals for each group; ***P < 0.001 vs sham, ###P < 0.001 vs VaD.

role in the neuroinflammation involved in the induction and evolution of neurodegenerative diseases by generating ROS and proinflammatory cytokines (Wang et al., 2015). In addition, the anomalous expression of cytoskeletal proteins such as MAP-2 and the activation of astrocytes are known to be closely associated with neuronal cell death (D'Andrea et al., 2001). Thus, we valued the effect of PEA-OXA on MAP-2 distribution, astrocytes and microglia activation after VaD induction. Treatment with PEA-OXA significantly reduced VaD-induced MAP-2 alteration and strongly limited the activation of GFAP and Iba-1.

Reactive astrogliosis could also be involved in the activation of the proinflammatory nuclear factor (NF)-κB pathway, and the inhibition of this pathway may confer protection against axonal loss, help to preserve white matter integrity and cognitive function (Saggu et al., 2016). Neuronal expression of NF-κB is stimulated by a multiplicity of insults, including TNF-α and mechanical injury, and is correlated with the subsequent expression of inflammatory mediators such as iNOS and COX-2 (Massa et al., 2006; Yune et al., 2004). NF-κB is normally isolated in the cytoplasm, bound to inhibitor protein IκBs. In response to stimuli including oxidative stress and inflammation, IκB is phosphorylated by IκB kinase (Bowie and O'Neill, 2000). This triggers the release of the NF-κB dimer, which can go into the nucleus. Accordingly, after VaD, we observed an increased IκB-α degradation and nuclear NF-κB translocation. PEA-OXA treatment significantly reduced IκB-α degradation as well as nuclear NF-κB translocation. By inhibiting the NF-κB pathway, PEA-OXA was also able to decrease the expression of iNOS and COX-2, as well as to increase the release of anti-inflammatory cytokines such as IL-10.

Studies have denoted that oxidative stress plays a critical role in the pathological process of stroke (Lastres-Becker et al., 2014). Since Nrf2 is a master controller of cytoprotective regulators against oxidative stress, the improved cognitive deficits and ischemic injury after PEA-OXA treatment could be due to an increase in Nrf2 activation. A previous study has in fact demonstrated that the activation of Nrf-2 and HO-1 could limit the infiltration of microglia in the pathological process of neurodegenerative diseases (Lastres-Becker et al., 2014).

Nrf2 is ubiquitously present in all human tissues and under basal conditions is negatively controlled in the cytoplasm by kelch-like ECH associating protein 1 (Keap1). Upon interruption of Keap1-Nrf2 binding, Nrf2 can transfer to the nucleus and coordinate the transcription of genes involved in antioxidant defense, such as Mn-SOD and HO-1 (Motohashi and Yamamoto, 2004; Wu et al., 2003). Expression of Nrf-2, as well as of Mn-SOD and HO-1, significantly decreased after VaD induction compared with control mice, whereas PEA-OXA treatment significantly upregulated levels of Nrf-2, as well as Mn-SOD and HO-1. Thus, the present study showed that PEA-OXA exerted neuroprotective effects dependent on Nrf2-mediated anti-oxidative pathways in models of VaD. PEA-OXA could protect against VaD by enhancing nuclear translocation of Nrf2 in neurons, upregulating the expression of Nrf2 and Nrf2 target genes; this was in agreement with our previous study of the MPTP model (Cordaro et al., 2018).

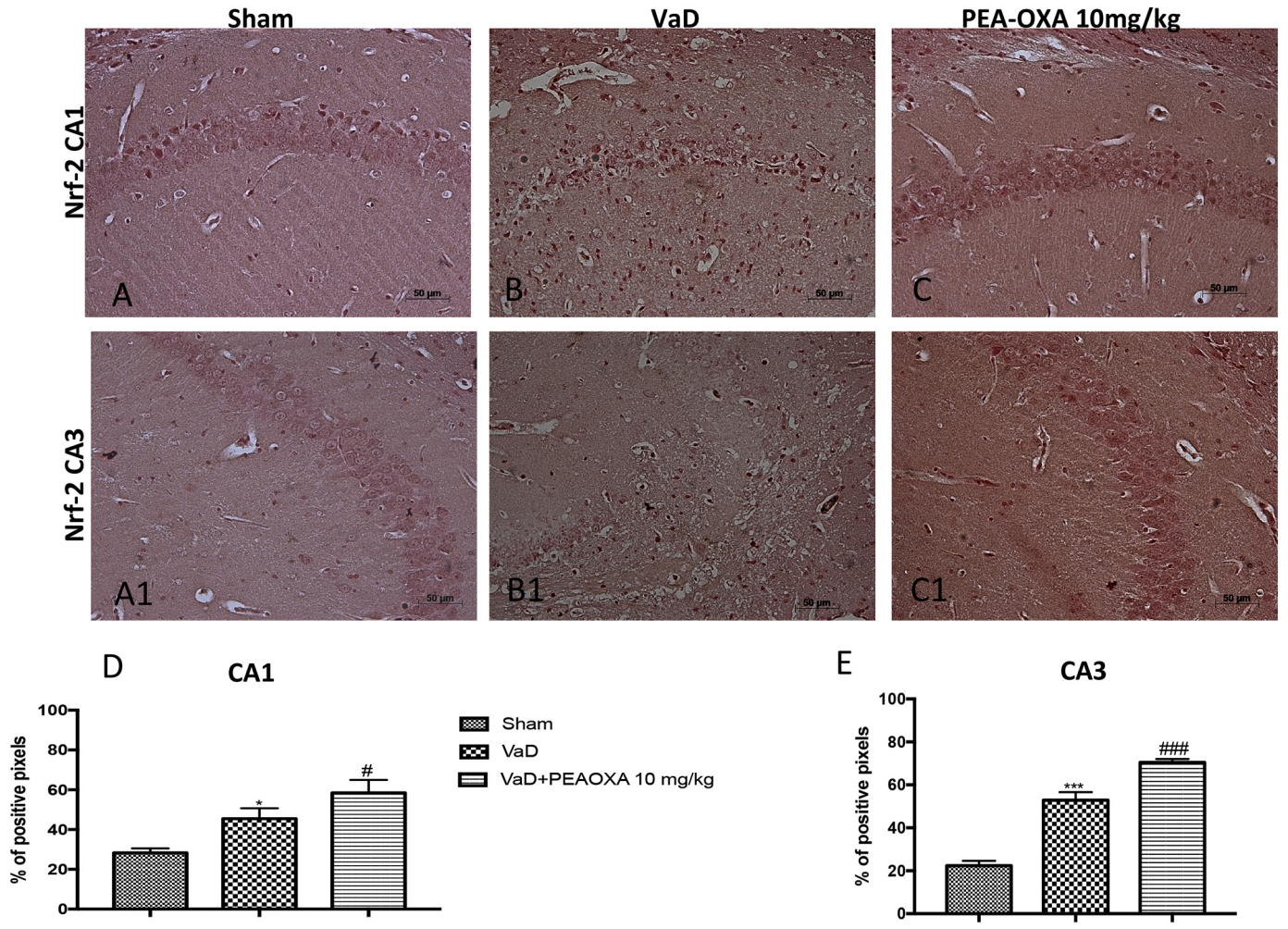

Fig. 9. Imunohistochemistry for NRF-2 after VaD induction.
Immunohistochemistry for NRF-2 in CA1 and CA3 regions respectively (A, A1) sham group, (B, B1) VaD + vehicle group, (C, C1) VaD + PEA-OXA group. The results are expressed as % of positive cells (D). Figures are representative of at least three independent experiments. Values are means ± SEM of 5 animals for each group; *P < 0.05 vs sham ***P < 0.001 vs sham, #P < 0.05 vs VaD. ###P < 0.001 vs VaD.

Apoptosis is an important type of active cell death and a key cause of pyramidal neuron loss. It results from cytoplasmic condensation, pyknotic nuclei, and DNA fragmentation, which can be detected by TUNEL staining. Researchers have reported that chronic cerebral hypoperfusion could promote apoptosis (Liu et al., 2017). In our study, we observed an increased number of apoptotic cells, together with an increased expression of proapoptotic markers such as BAX and decreased antiapoptotic marker Bcl-2 in VaD-subjected animals. This was reversed by PEA-OXA treatment. Hence, we demonstrated that PEA-OXA could ameliorate cognitive deficits by lessening neuron apoptosis in the hippocampus and ROS release, which are principal contributors to memory decline in dementia patients (Burke et al., 2014).

In conclusion, our data demonstrated that the neuroprotection of PEA-OXA in VaD operated via the regulation of important signaling pathways associated with oxidative stress, in particular by the inhibition of inflammatory NF-κB and activation of the antioxidant system, Nrf2. This research offers new insight into the mechanism of PEA-OXA-induced neuroprotection, suggesting a possible new therapeutic strategy to combat VaD. Thus, the modulation of intracellular NAAA by PEA-OXA treatment could signify a novel approach to control pathological conditions associated with neuroinflammation.

Conflict of interest statement

Salvatore Cuzzocrea is co-inventor on patent *WO2013/121449 A8 (Epitech Group SpA)*. Methods for the modulation of amidases capable of hydrolysing N-acylethanolamines useable in the therapy of inflammatory diseases. Moreover, Dr. Cuzzocrea is also a co-inventor with Epitech group on the following patents:

1. *EP 2814489*
2. *EP 2821083*
3. *EP 2985037*
4. *102015000067344*

No other authors have conflict of interests.

Source of funding

This research did not receive any specific grant from funding agencies in the public, commercial, or not-for-profit sectors.

Acknowledgments

The authors would like to thank Maria Antonietta Medici for excellent technical assistance, Miss Valentina Malvagni for editorial

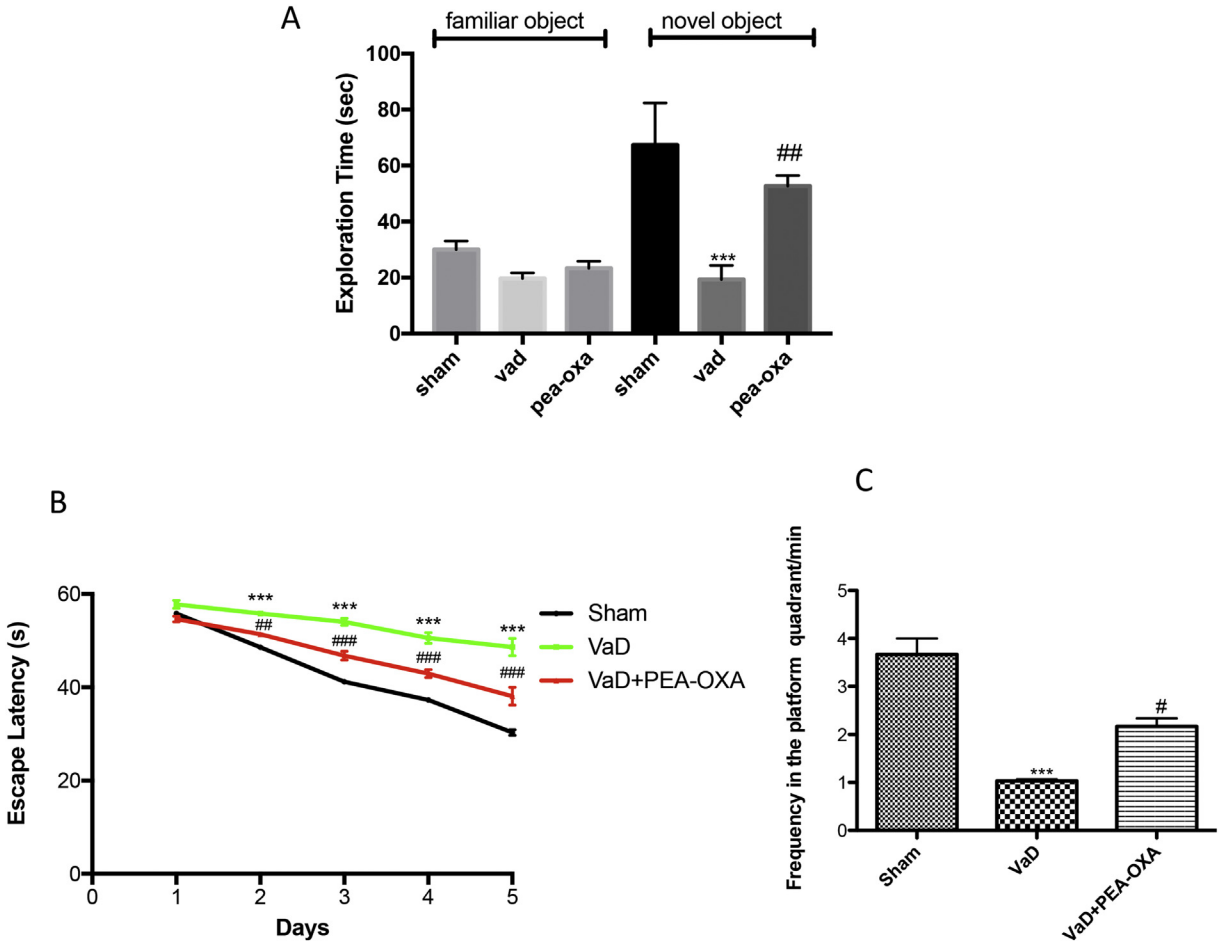

Fig. 10. PEA-OXA treatment on behavioral deficits after VaD induction.
Novel Object Recognition (NOR) and Morris Water maze (MWM) tests were evaluated. (A) Exploration time in *sec*; (B) Escape latency; (C) frequency in the platform quadrant/min. PEA-OXA treatment was able to increase the exploration time for the novel object recognition compared to vehicle group (A); to increase the time to found the platform (B) as well as the frequency time around and within the target quadrant of the platform (C) compared to controls. Values are means ± SEM of 10 animals for each group; ***P < 0.001 vs sham, #P < 0.05 vs VaD. ##P < 0.01 vs VaD ###P < 0.001 vs VaD.

support and Mr. Francesco Soraci for secretarial and administrative assistance.

References

Ahmad, A., et al., 2012a. Administration of palmitoylethanolamide (PEA) protects the neurovascular unit and reduces secondary injury after traumatic brain injury in mice. Brain Behav. Immun. 26, 1310–1321.
Ahmad, A., et al., 2012b. Reduction of ischemic brain injury by administration of palmitoylethanolamide after transient middle cerebral artery occlusion in rats. Brain Res. 1477, 45–58.
Alhouayek, M., Muccioli, G.G., 2014. Harnessing the anti-inflammatory potential of palmitoylethanolamide. Drug Discov. Today 19, 1632–1639.
Bar, K.J., et al., 2003. Pentosidine and N(epsilon)-(carboxymethyl)-lysine in Alzheimer's disease and vascular dementia. Neurobiol. Aging 24, 333–338.
Benito, C., et al., 2012. Beta-Amyloid exacerbates inflammation in astrocytes lacking fatty acid amide hydrolase through a mechanism involving PPAR-alpha, PPAR-gamma and TRPV1, but not CB(1) or CB(2) receptors. Br. J. Pharmacol. 166, 1474–1489.
Bisogno, T., et al., 1997. Biosynthesis, uptake, and degradation of anandamide and palmitoylethanolamide in leukocytes. J. Biol. Chem. 272, 3315–3323.
Bowie, A., O'Neill, L.A., 2000. Oxidative stress and nuclear factor-kappaB activation: a reassessment of the evidence in the light of recent discoveries. Biochem. Pharmacol. 59, 13–23.
Buckley, C.D., et al., 2013. The resolution of inflammation. Nat. Rev. Immunol. 13, 59–66.
Burke, M.J., et al., 2014. Morphometry of the hippocampal microvasculature in post-stroke and age-related dementias. Neuropathol. Appl. Neurobiol. 40, 284–295.
Choi, B.R., et al., 2011. Synergistic memory impairment through the interaction of chronic cerebral hypoperfusion and amlyloid toxicity in a rat model. Stroke 42, 2595–2604.
Cordaro, M., et al., 2017. Effects of a co-micronized composite containing palmitoylethanolamide and polydatin in an experimental model of benign prostatic hyperplasia. Toxicol. Appl. Pharmacol. 329, 231–240.
Cordaro, M., et al., 2018. 2-Pentadecyl-2-oxazoline reduces neuroinflammatory environment in the MPTP model of Parkinson disease. Mol. Neurobiol. 55 (12), 9251–9266.
Craft, S., 2009. The role of metabolic disorders in Alzheimer disease and vascular dementia two roads converged. Arch. Neurol. 66, 300–305.
Crunkhorn, S., 2012. Deal watch: Abbott boosts investment in NRF2 activators for reducing oxidative stress. Nat. Rev. Drug Discov. 11, 96.
D'Andrea, M.R., et al., 2001. Abnormal patterns of microtubule-associated protein-2 (MAP-2) immunolabeling in neuronal nuclei and Lewy bodies in Parkinson's disease substantia nigra brain tissues. Neurosci. Lett. 306, 137–140.
Driessler, F., et al., 2004. Molecular mechanisms of interleukin-10-mediated inhibition of NF-kappaB activity: a role for p50. Clin. Exp. Immunol. 135, 64–73.
Esposito, E., et al., 2014. Roles of fatty acid ethanolamides (FAE) in traumatic and ischemic brain injury. Pharmacol. Res. 86, 26–31.
Esposito, E., et al., 2016. A new co-micronized composite containing palmitoylethanolamide and polydatin shows superior oral efficacy compared to their association in a rat paw model of carrageenan-induced inflammation. Eur. J. Pharmacol. 782, 107–118.
Favaloro, B., et al., 2012. Role of apoptosis in disease. Aging (Albany NY) 4, 330–349.
Fidaleo, M., et al., 2014. Neuroprotective properties of peroxisome proliferator-activated receptor alpha (PPARalpha) and its lipid ligands. Curr. Med. Chem. 21, 2803–2821.
Fujii, M., et al., 1997. Strain-related differences in susceptibility to transient forebrain ischemia in SV-129 and C57Black/6 mice. Stroke 28, 1805–1810.
Hoyer, F.F., et al., 2014. Inhibition of endocannabinoid-degrading enzyme fatty acid amide hydrolase increases atherosclerotic plaque vulnerability in mice. J. Mol. Cell. Cardiol. 66, 126–132.
Impellizzeri, D., et al., 2014. Micronized/ultramicronized palmitoylethanolamide displays superior oral efficacy compared to nonmicronized palmitoylethanolamide in a rat model of inflammatory pain. J. Neuroinflammation 11, 136.
Impellizzeri, D., et al., 2016. 2-pentadecyl-2-oxazoline: Identification in coffee, synthesis and activity in a rat model of carrageenan-induced hindpaw inflammation. Pharmacol. Res. 108, 23–30.

Impellizzeri, D., et al., 2017. N-Palmitoylethanolamine-oxazoline as a new therapeutic strategy to control neuroinflammation: neuroprotective effects in experimental models of spinal cord and brain injury. J. Neurotrauma 34, 2609–2623.
Janda, E., et al., 2015. Parkinsonian toxin-induced oxidative stress inhibits basal autophagy in astrocytes via NQO2/quinone oxidoreductase 2: Implications for neuroprotection. Autophagy 11, 1063–1080.
Lastres-Becker, I., et al., 2014. Fractalkine activates NRF2/NFE2L2 and heme oxygenase 1 to restrain tauopathy-induced microgliosis. Brain 137, 78–91.
Li, Y., et al., 2012. Design and synthesis of potent N-acylethanolamine-hydrolyzing acid amidase (NAAA) inhibitor as anti-inflammatory compounds. PLoS ONE 7, e43023.
Liu, Z., et al., 2017. Cerebrolysin alleviates cognitive deficits induced by chronic cerebral hypoperfusion by increasing the levels of plasticity-related proteins and decreasing the levels of apoptosis-related proteins in the rat hippocampus. Neurosci. Lett. 651, 72–78.
Ma, X., et al., 2017. Salvianolic acid B ameliorates cognitive deficits through IGF-1/Akt pathway in rats with vascular dementia. Cell. Physiol. Biochem. 43, 1381–1391.
Magalhaes, C.A., et al., 2017. Alzheimer's disease and cytokine IL-10 gene polymorphisms: is there an association? Arq. Neuropsiquiatr. 75, 649–656.
Marsicano, G., et al., 2002. The endogenous cannabinoid system controls extinction of aversive memories. Nature 418, 530–534.
Massa, P.T., et al., 2006. NFkappaB in neurons? The uncertainty principle in neurobiology. J. Neurochem. 97, 607–618.
Mattace Raso, G., et al., 2014. Palmitoylethanolamide in CNS health and disease. Pharmacol. Res. 86, 32–41.
Motohashi, H., Yamamoto, M., 2004. Nrf2-Keap1 defines a physiologically important stress response mechanism. Trends Mol. Med. 10, 549–557.
Narayanan, S.V., et al., 2015. Resveratrol preconditioning protects against cerebral ischemic injury via nuclear erythroid 2-related factor 2. Stroke 46, 1626–1632.
Paterniti, I., et al., 2013. A new co-ultramicronized composite including palmitoylethanolamide and luteolin to prevent neuroinflammation in spinal cord injury. J. Neuroinflammation 10, 91.
Petrosino, S., et al., 2017. 2-Pentadecyl-2-oxazoline, the oxazoline of pea, modulates carrageenan-induced acute inflammation. Front. Pharmacol. 8, 308.
Piomelli, D., Sasso, O., 2014. Peripheral gating of pain signals by endogenous lipid mediators. Nat. Neurosci. 17, 164–174.
Purnell, C., et al., 2009. Cardiovascular risk factors and incident Alzheimer disease: a systematic review of the literature. Alzheimer Dis. Assoc. Disord. 23, 1–10.
Ribeiro, A., et al., 2015. A potent systemically active N-acylethanolamine acid amidase inhibitor that suppresses inflammation and human macrophage activation. ACS Chem. Biol. 10, 1838–1846.
Rivera, P., et al., 2015. Pharmacological blockade of the fatty acid amide hydrolase (FAAH) alters neural proliferation, apoptosis and gliosis in the rat hippocampus, hypothalamus and striatum in a negative energy context. Front. Cell. Neurosci. 9, 98.
Roman, G.C., 2002. Vascular dementia revisited: diagnosis, pathogenesis, treatment, and prevention. Med. Clin. North Am. 86, 477–499.
Saggu, R., et al., 2016. Astroglial NF-kB contributes to white matter damage and cognitive impairment in a mouse model of vascular dementia. Acta Neuropathol. Commun. 4, 76.
Sasso, O., et al., 2013. Antinociceptive effects of the N-acylethanolamine acid amidase inhibitor ARN077 in rodent pain models. Pain 154, 350–360.
Saturnino, C., et al., 2010. Synthesis and biological evaluation of new potential inhibitors of N-acylethanolamine hydrolyzing acid amidase. Bioorg. Med. Chem. Lett. 20, 1210–1213.
Sawant, S., et al., 2016. Prognostic role of Oct4, CD44 and c-Myc in radio-chemo-resistant oral cancer patients and their tumourigenic potential in immunodeficient mice. Clin. Oral Investig. 20, 43–56.
Seitz, D.P., et al., 2011. Antidepressants for agitation and psychosis in dementia. Cochrane Database Syst. Rev. CD008191.
Sekhon, L.H., et al., 1997. Chronic cerebral hypoperfusion: pathological and behavioral consequences. Neurosurgery 40, 548–556.
Siegmund, S.V., et al., 2013. Fatty acid amide hydrolase but not monoacyl glycerol lipase controls cell death induced by the endocannabinoid 2-arachidonoyl glycerol in hepatic cell populations. Biochem. Biophys. Res. Commun. 437, 48–54.
Siracusa, R., et al., 2017. Anti-inflammatory and neuroprotective effects of co-ultraPEALut in a mouse model of vascular dementia. Front. Neurol. 8, 233.
Skaper, S.D., et al., 2015. N-Palmitoylethanolamine and neuroinflammation: a novel therapeutic strategy of resolution. Mol. Neurobiol. 52, 1034–1042.
Solorzano, C., et al., 2009. Selective N-acylethanolamine-hydrolyzing acid amidase inhibition reveals a key role for endogenous palmitoylethanolamide in inflammation. Proc. Natl. Acad. Sci. U. S. A. 106, 20966–20971.
Thimmulappa, R.K., et al., 2006. Nrf2 is a critical regulator of the innate immune response and survival during experimental sepsis. J. Clin. Invest. 116, 984–995.
Todorovic, M., et al., 2016. Nrf2: a modulator of Parkinson's disease? J. Neural Transm. (Vienna) 123, 611–619.
Toyama, K., et al., 2014. Apoptosis signal-regulating kinase 1 is a novel target molecule for cognitive impairment induced by chronic cerebral hypoperfusion. Arterioscler. Thromb. Vasc. Biol. 34, 616–625.
Ueda, N., et al., 2010. N-acylethanolamine metabolism with special reference to N-acylethanolamine-hydrolyzing acid amidase (NAAA). Prog. Lipid Res. 49, 299–315.
Varghese, F., et al., 2014. IHC Profiler: an open source plugin for the quantitative evaluation and automated scoring of immunohistochemistry images of human tissue samples. PLoS ONE 9, e96801.
Wang, H., 2014. Establishment of an animal model of vascular dementia. Exp. Ther. Med. 8, 1599–1603.
Wang, X.R., et al., 2015. Acupuncture ameliorates cognitive impairment and hippocampus neuronal loss in experimental vascular dementia through Nrf2-mediated antioxidant response. Free Radic. Biol. Med. 89, 1077–1084.
Wu, D.C., et al., 2003. NADPH oxidase mediates oxidative stress in the 1-methyl-4-phenyl-1,2,3,6-tetrahydropyridine model of Parkinson's disease. Proc. Natl. Acad. Sci. U. S. A. 100, 6145–6150.
Xiong, Z., et al., 2017. Dl-3-n-butylphthalide treatment enhances hemodynamics and ameliorates memory deficits in rats with chronic cerebral hypoperfusion. Front. Aging Neurosci. 9, 238.
Yamano, Y., et al., 2012. Lipophilic amines as potent inhibitors of N-acylethanolamine-hydrolyzing acid amidase. Bioorg. Med. Chem. 20, 3658–3665.
Yang, L., et al., 2015. Potential analgesic effects of a novel N-acylethanolamine acid amidase inhibitor F96 through PPAR-alpha. Sci. Rep. 5, 13565.
Yune, T.Y., et al., 2004. Manganese superoxide dismutase induced by TNF-beta is regulated transcriptionally by NF-kappaB after spinal cord injury in rats. J. Neurotrauma 21, 1778–1794.
Zhen, J., et al., 2014. Effects of grape seed proanthocyanidin extract on pentylenetetrazole-induced kindling and associated cognitive impairment in rats. Int. J. Mol. Med. 34, 391–398.